

Reflected multi-entropy and its holographic dual

Ma-Ke Yuan,^{1,*} Mingyi Li,^{1,†} and Yang Zhou^{1,‡}

¹*Department of Physics and Center for Field Theory and Particle Physics, Fudan University, Shanghai 200433, China*

We introduce a mixed-state generalization of the multi-entropy through the canonical purification, which we called reflected multi-entropy. We propose the holographic dual of this measure. For the tripartite case, a field-theoretical calculation is performed using a six-point function of twist operators at large c limit. At both zero and finite temperature, the field-theoretical results match the holographic results exactly, supporting our holographic conjecture of this new measure.

I. INTRODUCTION

Quantum entanglement [1, 2] has recently emerged as a key tool in understanding the AdS/CFT correspondence [3–5], which remains one of our most successful frameworks for probing quantum gravity. Remarkably, the Ryu-Takayanagi formula [6–9] provides a means to calculate entanglement entropy in conformal field theories (CFTs) via the minimal area of a codimension-2 surface in anti-de Sitter (AdS) space, establishing a precise link between spacetime geometry and quantum entanglement. However, entanglement entropy exclusively captures quantum entanglement for pure states. To extend this connection to mixed states, holographic duals for several other measures, such as the entanglement of purification [10–12], reflected entropy [13–15], logarithmic negativity [16–20], and also odd entanglement entropy [21, 22], have recently been studied. Another important direction lies in the investigation of multipartite correlation measures [23–30] and their holographic duals play a critical role in understanding the emergence of bulk spacetime from many-body quantum entanglement on the boundary. The aim of this letter is to bridge the gap between multipartite correlations in mixed states and spacetime geometry. The multipartite entanglement of purification has been investigated in [31, 32] and the multipartite generalization of reflected entropy has been studied in [33, 34].

For a given multipartite mixed state, we can canonically purify it to obtain a pure state [13]. Using the recent proposal for pure state multipartite entanglement measure [35] based on the replica trick and permutation invariance, one can compute the so-called multi-entropy for the purified state. We propose this as an intrinsic multipartite measure for the original mixed state, which we term *reflected multi-entropy*. Unlike multi-entropy [36–39], reflected multi-entropy is intrinsically well-defined in the ultraviolet, thus circumventing the divergence issue that plagues entanglement entropy as well as multi-entropy in QFT. In the remainder of this letter, we first introduce reflected multi-entropy as the mixed-state generalization of multi-entropy, and then propose its holo-

graphic dual. For the tripartite case, we perform a field-theoretical calculation using a six-point function of twist operators and find that it matches the holographic result exactly, both at zero and finite temperature.

II. A GENERALIZATION OF MULTI-ENTROPY

A. Review of multi-entropy

Let us recall some basic notions of entanglement entropy (EE) and Rényi entropy. Given a pure state $|\psi\rangle_{AB}$ that describes two systems A and B , the EE between A and B is defined as

$$S(A) = -\text{Tr} \rho_A \log \rho_A, \quad (1)$$

where $\rho_A = \text{Tr}_B |\psi\rangle\langle\psi|_{AB}$ is the reduced density matrix. Rényi entropy is a one-parameter generalization of EE

$$S_n(A) = \frac{1}{1-n} \log \text{Tr} \rho_A^n, \quad (2)$$

which reduces to EE (1) in the limit $n \rightarrow 1$. This is called *replica trick*. In order to introduce the multi-entropy, let us reformulate ρ_A^n through the permutation and contraction of the indices of the n copies of ρ_A ,

$$\begin{aligned} \rho_A^n &= (\rho_A)_{\alpha_1}^{\alpha_2} (\rho_A)_{\alpha_2}^{\alpha_3} (\rho_A)_{\alpha_3}^{\alpha_4} \cdots (\rho_A)_{\alpha_{n-1}}^{\alpha_n} \\ &= (\rho_A)_{\alpha_1}^{\alpha_{\sigma \cdot 1}} (\rho_A)_{\alpha_2}^{\alpha_{\sigma \cdot 2}} (\rho_A)_{\alpha_3}^{\alpha_{\sigma \cdot 3}} \cdots (\rho_A)_{\alpha_n}^{\alpha_{\sigma \cdot n}}, \end{aligned} \quad (3)$$

with $\sigma = (123 \cdots n)$ the permutation acting on the index of replicas. Guided by this key observation, in [35] the authors defined the *multi-entropy* $S^{(q)}$, which generalizes the concept of EE to q -partite cases through the permutation and contraction of indices. Let us focus on tripartite pure state $|\psi\rangle_{ABC}$ to illustrate.

Like Rényi entropy, the entanglement measure $S_n^{(q=3)}$ should be determined by the choice of permutation $(\sigma_A, \sigma_B, \sigma_C)$ acting on the indices of different replicas, i.e., the way of contracting multiple density matrices. Note that there is a equivalence relation

$$(\sigma_A, \sigma_B, \sigma_C) \sim (\sigma_A, \sigma_B, \sigma_C) \cdot g \quad (4)$$

allowing us to consider only $(q-1)$ -parties, i.e., we can always choose $g = \sigma_A^{-1}$ to make $\sigma_A = \text{id}$ and the entanglement measure is only determined by (σ_B, σ_C) .¹ Both B

* mkyuan19@fudan.edu.cn

† limy22@m.fudan.edu.cn

‡ yang.zhou@fudan.edu.cn

¹ In this letter, we treat all the subsystems symmetrically.

and C have n replicas and (σ_B, σ_C) are chosen to be cyclic permutations of order n . In total, we have $n^{q-1} = n^2$ replicas, which form a $n \times n$ square lattice. The multi-entropy is defined by choosing the replica symmetry as $\mathbb{Z}_n \otimes \mathbb{Z}_n$ with the first/second \mathbb{Z}_n acting on the subregion B/C and cyclically permuting the replicas located in the same row/column of the lattice.

For general n and q -partite entanglement, the Rényi multi-entropy is defined as²

$$S_n^{(q)} = \frac{1}{1-n} \log \left(\mathcal{Z}_{n^{q-1}}^{(q)} / (\mathcal{Z}_1^{(q)})^{n^{q-1}} \right), \quad (5)$$

where $\mathcal{Z}_{n^{q-1}}^{(q)}$ is the partition function on the n^{q-1} -sheet Riemann surface with replica symmetry $\mathbb{Z}_n^{\otimes(q-1)}$ as described above. The multi-entropy is defined by taking the $n \rightarrow 1$ limit

$$S^{(q)} = \lim_{n \rightarrow 1} S_n^{(q)}. \quad (6)$$

For $q = 3$ and $n = 2$, the partition function contains 4 replicas with the gluing $\sigma_B = (13)(24)$ and $\sigma_C = (12)(34)$ as illustrated in FIG. 1 via the Euclidean path integral [40–42]. This results in a contraction of four density

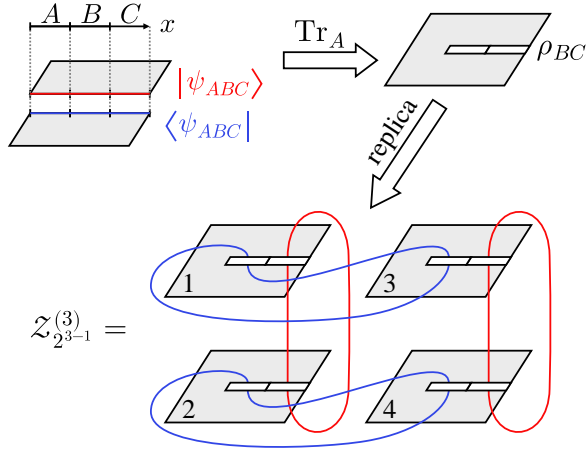


FIG. 1. The construction of the n^{q-1} -sheet Riemann surface in the special case $q = 3$ and $n = 2$.

matrices (here we abbreviate ρ_{BC} as ρ)

$$\mathcal{Z}_{2^{3-1}}^{(3)} = \rho_{\beta_1 \chi_1}^{\beta_3 \chi_2} \rho_{\beta_2 \chi_2}^{\beta_4 \chi_1} \rho_{\beta_3 \chi_3}^{\beta_1 \chi_2} \rho_{\beta_4 \chi_4}^{\beta_2 \chi_3}. \quad (7)$$

The corresponding Rényi multi-entropy is given by

$$S_2^{(3)} = \frac{1}{1-2} \log \left(\mathcal{Z}_{2^{3-1}}^{(3)} / (\mathcal{Z}_1^{(3)})^{2^{3-1}} \right), \quad (8)$$

with $\mathcal{Z}_1^{(3)} = \rho_{\beta \chi}^{\beta \chi}$ serving as the normalization factor.

² Compared with [35], we use a slightly different notation here. We denote the partition function on the n^{q-1} -sheet Riemann surface by $\mathcal{Z}_{n^{q-1}}^{(q)}$ instead of $\mathcal{Z}_n^{(q)}$ in [35].

B. Mixed-state generalization of multi-entropy through canonical purification

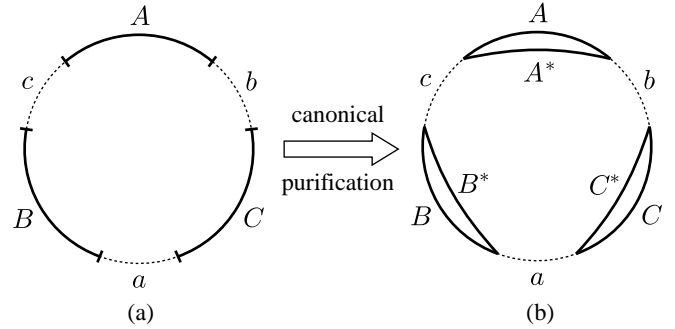


FIG. 2. Canonical purification of ρ_{ABC} . (a) Global pure state ψ_{AcBaCb} defined on a circle. Tracing out abc gives a mixed state ρ_{ABC} . (b) Picking up another copy of ρ_{ABC} and gluing these two copies along abc gives a big pure state $|\sqrt{\rho_{ABC}}\rangle$ (9), which is the canonical purification of ρ_{ABC} .

A multipartite mixed state can be obtained by tracing out some part from a pure state. Again we will focus on tripartite case with $q = 3$ but it can be generalized to larger q straightforwardly. Starting from a pure state $\psi_{AcBaCb} \in \mathcal{H}_{AcBaCb}$ and tracing out abc , we obtain a mixed state ρ_{ABC} , which can be canonically purified by doubling the Hilbert space (see FIG. 2 for a schematic diagram of this purification process). For more discussions on canonical purification we refer to [13]. The purified state can be expressed as

$$|\sqrt{\rho_{ABC}}\rangle = |\sqrt{\text{Tr}_{abc} |\psi_{AcBaCb}\rangle \langle \psi_{AcBaCb}|}| \in (\mathcal{H}_A \otimes \mathcal{H}_A^*) \otimes (\mathcal{H}_B \otimes \mathcal{H}_B^*) \otimes (\mathcal{H}_C \otimes \mathcal{H}_C^*). \quad (9)$$

We define the *reflected multi-entropy* as

$$S_R^{(q=3)}(A; B; C) = S^{(q=3)}(AA^*; BB^*; CC^*)|_{|\sqrt{\rho_{ABC}}\rangle}, \quad (10)$$

with $S^{(q)}$ the original multi-entropy (6). The subscript R of $S_R^{(q)}$ denotes “reflected”.³

Here we list some properties of reflected multi-entropy,

(i) It reduces to twice the multi-entropy for pure state $\rho_{AB\dots} = |\psi\rangle \langle \psi|_{AB\dots}$,

$$\text{pure state: } S_R^{(q)}(A; B; \dots) = 2S^{(q)}(A; B; \dots). \quad (11)$$

(ii) It reduces to the reflected entropy [13] for bipartite system ρ_{AB} ,

$$\text{bipartite case: } S_R^{(q=2)}(A; B) = S_R(A; B). \quad (12)$$

³ The marriage with holographic purification was also mentioned in [36] without explicit construction.

- (iii) For factorized density matrix $\rho_{AB\dots} = \rho_A \otimes \rho_B \otimes \dots$, $S_R^{(q)}(A; B; \dots)$ vanishes,

$$\text{factorized state: } S_R^{(q)}(A; B; \dots) = 0. \quad (13)$$

- (iv) $S_R^{(q)}(A; B; \dots)$ is bounded from below by multi-entropy of purification,

$$\text{lower bound: } S_R^{(q)}(A; B; \dots) \geq M_P(A; B; \dots), \quad (14)$$

where the multi-entropy of purification M_P is defined by minimization of multi-entropy over all possible purifications.

- (v) $S_R^{(q)}(A; B; \dots)$ is bounded from below by half the multipartite reflected entropy [34] for holographic states,

$$\text{lower bound: } S_R^{(q)}(A; B; \dots) \geq \frac{1}{2} \Delta_R(A; B; \dots). \quad (15)$$

III. HOLOGRAPHY OF REFLECTED MULTI-ENTROPY

In the previous section we introduced the reflected multi-entropy as a multipartite measure for mixed states. Based on the canonical purification for holographic states [13] and the holographic proposal for multi-entropy [35], now we want to find the holographic dual for reflected multi-entropy. Consider a global pure state ψ_{AcBaCb} defined on a circle as show in FIG. 2(a). This pure state has a classical bulk solution as its holographic dual. Now we trace out abc , which corresponds to retaining only the entanglement wedge for ρ_{ABC} and prescinding other portion of the bulk. To perform the canonical purification, we pick up another copy of the entanglement wedge and glue these two copies along Γ_{ABC} , the Ryu-Takayanagi surface (RT surface) for ρ_{ABC} . The resulting geometry is drawn in FIG. 3(a).

To figure out the geometry dual of the reflected multi-entropy defined in subsection II B, which now becomes the multi-entropy between AA^* , BB^* and CC^* , we need to generalize the holographic proposal for multi-entropy [35] to multi-boundary pure states. Recall that the original holographic proposal for multi-entropy is a minimal bulk web \mathcal{W} consist of minimal codimension-2 surfaces. For a single boundary pure state, \mathcal{W} is anchored at the boundaries of all subsystems A, B, \dots . This condition is relaxed in the case of multi-boundary, much like the RT surfaces for multi-boundary states. Another important condition is that \mathcal{W} should contain sub-webs that are homologous to all the subsystems A, B, \dots . This can be easily satisfied. It is then natural to propose the holographic dual of the reflected multi-entropy as the minimal surface web shown in FIG. 3(a). The situation is similar for the four-partite case as drawn in FIG. 4, but now there are two channels and one should pick the minimum of them. More precisely, the holographic dual of

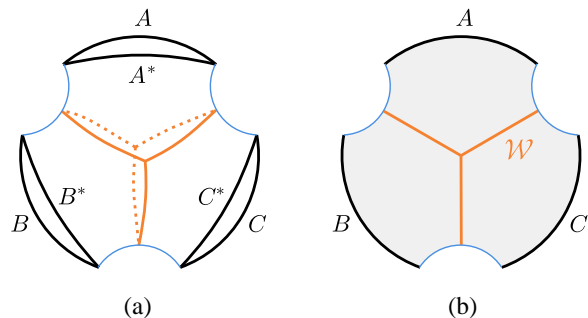


FIG. 3. (a) Canonical purification of ρ_{ABC} and its holographic dual. Tracing out abc corresponds to gluing along Γ_{ABC} , the RT surface for ρ_{ABC} (blue curves). The orange web \mathcal{W} is the minimal web in the bulk as the holographic dual of $S^{(3)}(AA^*; BB^*; CC^*)$. (b) The single copy picture. The shadow area is the entanglement wedge of $A \cup B \cup C$ and the orange web is the holographic dual of $S_R^{(3)}(A; B; C)$.

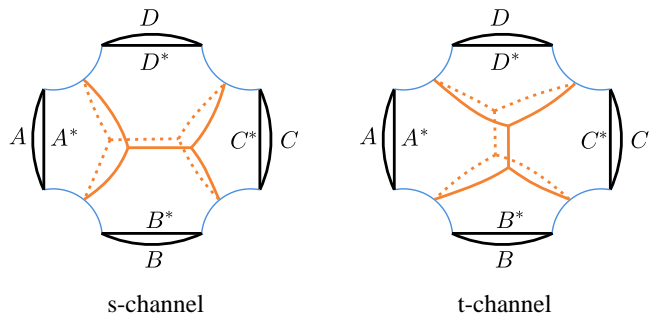


FIG. 4. Four-partite case.

the reflected multi-entropy $S_R^{(q)}(A; B; \dots)$ is the minimal surface web \mathcal{W} satisfying the following topological conditions:

- (1) \mathcal{W} is anchored at $\Gamma_{AB\dots}$ which is the RT surface of the system $A \cup B \cup \dots$.
- (2) \mathcal{W} contains sub-webs that are homologous to all the subsystems A, B, \dots .

The holographic reflected multi-entropy is computed by

$$S_R^{(q)} = \frac{2}{4G_N} \min_{\mathcal{W}} L[\mathcal{W}], \quad (16)$$

with $L[\mathcal{W}]$ the area of the web \mathcal{W} in a single copy as illustrated in FIG. 3(b).

IV. COMPUTATION IN $\text{AdS}_3/\text{CFT}_2$

A. Zero temperature case

Let us study a simple example in $\text{AdS}_3/\text{CFT}_2$, as illustrated in FIG. 5. We work in Poincaré half plane with

the metric

$$ds^2 = \frac{dx^2 + dy^2}{y^2}, \quad x \in (-\infty, +\infty) \text{ \& } y \in [0, +\infty). \quad (17)$$

We consider the reflected multi-entropy $S_R^{(3)}(A; B; C)$ between three subsystems A, B, C . ρ_{ABC} is a mixed state obtained by tracing out abc from the pure state ψ_{AcBaCb} defined on \mathbb{R} as shown in FIG. 5. The subsystems A, B, C are chosen to be

$$A = [x_1, x_2], \quad B = [x_3, x_4], \quad C = [x_5, x_6], \quad (18)$$

with $x_{i=1, \dots, 6}$ parameterized by $\xi = a, b, c$

$$\begin{aligned} x_6 &= -x_1 = b, \\ x_5 &= -x_2 = a + r, \\ x_4 &= -x_3 = a - r. \end{aligned} \quad (19)$$

In the following we will calculate $S_R^{(3)}(A; B; C)$ using both holographic method and field theoretical method and find the precise agreement.

1. Holographic calculation

As we have seen in section III, the holographic dual of $S_R^{(3)}(A; B; C)$ is given by the minimal web denoted by orange curves in FIG. 5. Due to the \mathbb{Z}_2 -symmetry about the $x = 0$ axis in FIG. 5, the junction I is expected to be on $x = 0$ and we denote it by $I(0, y_I)$. For general two points (x_1, y_1) and (x_2, y_2) on the Poincaré half plane, the distance between them is

$$D((x_1, z_1), (y_2, y_2)) = \operatorname{arccosh} \frac{(x_1 - x_2)^2 + y_1^2 + y_2^2}{2y_1 y_2}. \quad (20)$$

Therefore, the distance between I and a point $(-a + r \cos \phi, r \sin \phi)$ on the RT surface of c is

$$D((0, y_I), (-a + r \cos \phi, r \sin \phi)), \quad (21)$$

which should be minimized over ϕ . Similar distances between I and the RT surface of a, b can be worked out and we finally end up with the length of the bulk dual web

$$\begin{aligned} L[\mathcal{W}](a, b, r) &= \min_{y_I} \left[\log(b/y_I) \right. \\ &\quad \left. + 2 \operatorname{arcsech} \frac{2y_I r}{\sqrt{((a-r)^2 + y_I^2)((a+r)^2 + y_I^2)}} \right], \end{aligned} \quad (22)$$

where the first/second term in $[\dots]$ comes from the distance between I and the RT surface of $b/\{a, c\}$. In (22) we did not minimize over y_I and we will do that numerically when comparing with the field theory results (see the blue curves in FIG. 6).

2. Field theoretical calculation

In this subsection we calculate $S_R^{(3)}(A; B; C)$ in conformal field theory. Using the replica trick, we first represent the reflected multi-entropy as a path integral on a specific Riemann surface. The example for $\{q = 3, n = 3, m = 2\}$ is shown in FIG. 10. Here a new replica number m is introduced for canonical purification (see [13] and Appendix A for details).

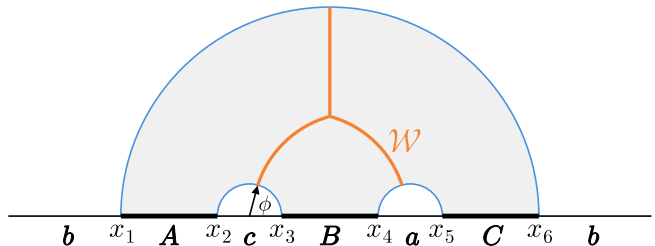


FIG. 5. The holographic dual of $S_R^{(q=3)}(A; B; C)$.

The n -th Rényi version of reflected multi-entropy is given by

$$S_R^{(q)}[n] = \frac{1}{1-n} \log \frac{\mathcal{Z}_{n^{q-1}, m}}{(\mathcal{Z}_{1, m})^{n^{q-1}}}, \quad (23)$$

and the reflected multi-entropy can be obtained by taking the limit $n \rightarrow 1$ and $m \rightarrow 1$

$$S_R^{(q)} = \lim_{m \rightarrow 1} \lim_{n \rightarrow 1} \frac{1}{1-n} \log \frac{\mathcal{Z}_{n^{q-1}, m}}{(\mathcal{Z}_{1, m})^{n^{q-1}}}. \quad (24)$$

Now we use the twist operator correlation function to express $\mathcal{Z}_{n^{q-1}, m}$, the path integral on a glued Euclidean spacetime with mn^{q-1} copies. The conformal weights h_i of twist operators $\sigma_i(x_i)$ are given by (see Appendix A for the derivation)

$$h_{i=1, \dots, 2q} = \frac{c}{24} \left(m - \frac{1}{m} \right) n^{q-1}. \quad (25)$$

When $q = 2$, one can check that (25) reduces to the conformal weight of the twist operators for the reflected entropy as we expected.⁴ The conformal weight h_a of the leading operators σ_a in OPE $\sigma_i(x_i)\sigma_j(x_j) \rightarrow \sigma_{a=ij}(x_a)$ are (see Appendix A for the derivation)

$$h_{a=ij} = \frac{c}{12} (n^{q-1} - n^{q-3}). \quad (26)$$

⁴ For reflected entropy, we have [13]

$$h_{g_A} = h_{g_A^{-1}} = \frac{cn(m^2 - 1)}{24m},$$

where g_A and g_A^{-1} are the twist operators located at the two endpoints of interval A .

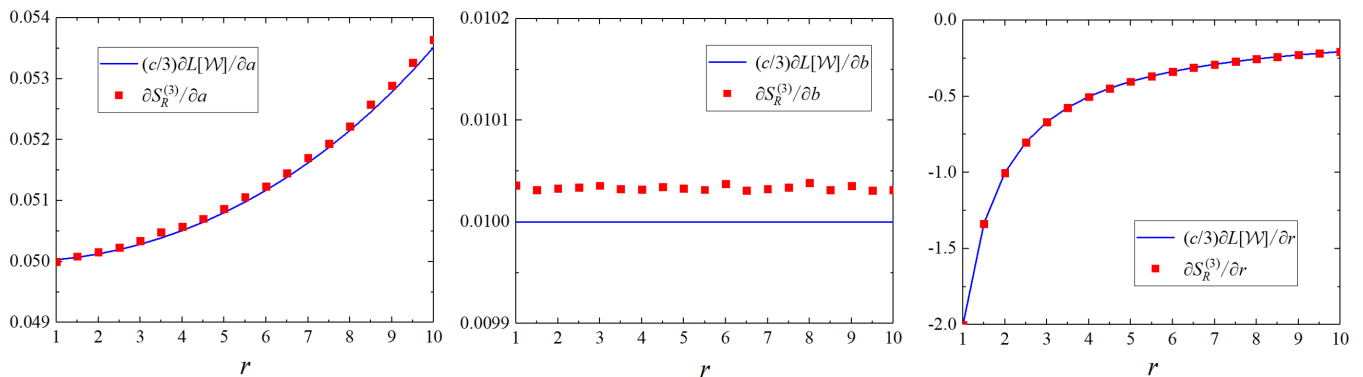


FIG. 6. Comparison of the partial derivatives of $\frac{c}{3}L[\mathcal{W}]$ and $S_R^{(q=3)}$ (divided by $c/3$) with respect to $\xi = a, b, r$. We take $a = 20$, $b = 100$ and r ranging from 1 to 10.

The conformal weight (26) is twice the conformal weight of the twist operators for the original multi-entropy as we expected.⁵ It can also be checked that taking $q = 2$, (26) reduces to twice of the conformal weight of the twist operators of EE.

Using these twist operators, $\mathcal{Z}_{n^{q-1}, m}$ can be represented by the six-point function

$$\mathcal{Z}_{n^{q-1}, m} = \langle \sigma_1 \sigma_2 \sigma_3 \sigma_4 \sigma_5 \sigma_6 \rangle_{\text{CFT}^{\otimes mn^{q-1}}}, \quad (27)$$

with σ_i located at x_i . At large c limit, the calculation of the six-point function (27) can be converted to solving a monodromy problem [43, 44], i.e., solving a second-order differential equation (B5) with specific boundary conditions (B8). Following the approach in [45] we numerically compute the six-point function (27) at large c limit (the details are included in Appendix B) and the partial derivatives of $S_R^{(3)}(A; B; C)$ with respect to a, b, r are plotted in FIG. 6.

On the other hand, the holographic result is given by minimizing $L[\mathcal{W}](a, b, r)$ in (22). The partial derivatives of $\frac{c}{3}L[\mathcal{W}](a, b, r)$ with respect to a, b, r are numerically plotted in FIG. 6 and compared with the field theoretical results. The two results match precisely.

B. Finite temperature case

In this subsection we consider reflected multi-entropy in CFT at finite temperature, the bulk dual of which is BTZ black hole [46]

$$ds^2 = \frac{1}{y^2} \left(f(y) d\tau^2 + \frac{dy^2}{f(y)} + dx^2 \right), \quad (28)$$

where $f(y) = 1 - (y/y_H)^2$ with $y = y_H$ the horizon as shown in FIG. 7, $\tau \sim \tau + 2\pi y_H$, $\beta_{\text{CFT}} = 2\pi y_H$, and

⁵ The conformal dimension of the twist operators of multi-entropy is given in eq(29) of [38].

we have set the AdS radius to be 1. To be specific, we consider the reflected multi-entropy among the following three intervals

$$A = [-b, -a], \quad B = [-a, a], \quad C = [a, b], \quad (29)$$

on the time slice $\tau = 0$ as illustrated in FIG. 7. To simplify, we consider the case that b goes to infinity.

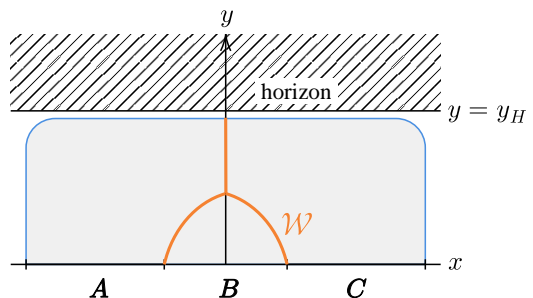


FIG. 7. The holographic dual of $S_R^{(q=3)}(A; B; C)$ at finite temperature.

1. Holographic calculation

Now we compute the holographic reflected multi-entropy in the presence of BTZ black hole. The distance between two arbitrary points (τ, x, y) and (τ', x', y') in the BTZ metric (28) is given by

$$\begin{aligned} & \tilde{D}((\tau, x, y), (\tau', x', y')) \\ &= \text{arccosh}(T_1 T'_1 + T_2 T'_2 - X_1 X'_1 - X_2 X'_2), \end{aligned} \quad (30)$$

with

$$\begin{aligned} T_1 &= \sqrt{\frac{y_H^2}{y^2} - 1} \sinh \frac{\tau}{y_H}, & T_2 &= \frac{y_H}{y} \cosh \frac{x}{y_H}, \\ X_1 &= \sqrt{\frac{y_H^2}{y^2} - 1} \cosh \frac{\tau}{y_H}, & X_2 &= \frac{y_H}{y} \sinh \frac{x}{y_H}. \end{aligned} \quad (31)$$

Due to the \mathbb{Z}_2 -symmetry about the $x = 0$ axis in FIG. 7, we denote the junction point I by $I(0, y_I)$. Since we send b to ∞ , the RT surface of $A \cup B \cup C$ will be very close to the horizon. Therefore, the sum of the total three geodesics is given by

$$2\tilde{D}((0, a, \epsilon), (0, 0, y_I)) + \tilde{D}((0, 0, y_H), (0, 0, y_I)) , \quad (32)$$

with ϵ the UV cutoff. Minimizing (32) with respect to y_I , we end up with $y_I = \frac{\sqrt{3}y_H \sinh(a/y_H)}{2 \cosh(a/y_H) - 1}$ and

$$L[\mathcal{W}](a) = \operatorname{arccosh} \frac{2 \cosh \frac{a}{y_H} - 1}{\sqrt{3} \sinh \frac{a}{y_H}} + 2 \log \frac{2y_H \left(2 \cosh^2 \frac{a}{y_H} - \left| \cosh \frac{a}{y_H} - 2 \right| - \cosh \frac{a}{y_H} \right)}{\sqrt{3} \epsilon \sinh \frac{a}{y_H}} . \quad (33)$$

2. Field theoretical calculation

From the CFT perspective, we need $\mathcal{Z}_{n^q-1, m}$, which can be obtained from the six-point function on a cylinder of infinite length with period β_{CFT}

$$\langle \sigma_1 \sigma_2 \sigma_3 \sigma_4 \sigma_5 \sigma_6 \rangle_{\text{cylinder}} , \quad (34)$$

with σ_i located at $\tau_i = 0$ and $x = x_i$, which is given by

$$\begin{aligned} x_6 &= -x_1 = b = \infty , \\ x_5 &= -x_2 = a + \epsilon , \\ x_4 &= -x_3 = a - \epsilon . \end{aligned} \quad (35)$$

The conformal weight of σ_i is given by (25) as before. To compute (34) we perform the conformal transformation (here $w_i = x_i + i\tau_i$)

$$z_i = 1 - \exp \frac{2\pi(w_2 - w_i)}{\beta_{\text{CFT}}} , \quad (36)$$

which sends $\{w_1, w_2, w_6\}$ to $\{\infty, 0, 1\}$ and $\{w_3, w_4, w_5\}$ to $\{z_3, z_4, z_5\}$. Following the same method in Appendix B, we can numerically evaluate the derivative of the reflected multi-entropy with respect to a and compare it with the holographic result (33) as plotted in FIG. 8. Again these two results match precisely.

V. DISCUSSION

In this letter we introduced reflected multi-entropy as a multipartite measure for mixed state by combining the recent proposal of multi-entropy and canonical purification. This is a new multipartite generalization of reflected entropy, in contrast to earlier attempts [33, 34] which only involve entanglement entropy and canonical purifications (possibly many times). Remarkably, reflected multi-entropy can be computed by replica trick in CFTs

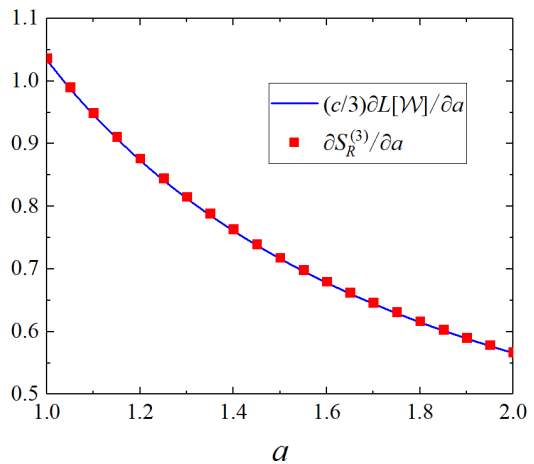


FIG. 8. The partial derivatives of $\frac{c}{3}L[\mathcal{W}]$ and $S_R^{(q=3)}$ (divided by $c/3$) with respect to a . We take $y_H = 5$, $b = 1000$, $\epsilon = 0.02$ and a ranging from 1 to 2.

at both zero temperature and finite temperature and we find precise match between CFT results and the holographic results. Our results strongly support a new class of duality between multipartite measures for mixed states and spacetime geometry. A couple of future questions are listed in order: First, it is straightforward to generalize our discussion to multiple canonical purifications. Any multi-entropy with different number of parties for the final pure state provides a multipartite measure for the original mixed state. Reflected multi-entropy is singled out for its simplicity. Second, generalize our holographic conjecture to time dependent cases. Since both reflected entropy and multi-entropy are expected to have covariant generalizations [13, 35], we expect that the covariant reflected multi-entropy is obtained as the area of the minimal extremal surface web rather than the global minimal one. Last but not least, it would be interesting to consider the bulk quantum corrections [47, 48] to our entropy to see if there is a sub-leading correction as a bulk reflected multi-entropy.

Acknowledgement. We are grateful for useful discussions with our group members in Fudan University. We would like to thank Jinwei Chu for helpful discussions. This work is supported by NSFC grant 12375063. This work is also sponsored by Natural Science Foundation of Shanghai (21ZR1409800) as well as Shanghai Talent Development Fund.

Appendix A: Derivation of conformal weights (25) and (26)

In this appendix we derive the conformal weights (25) and (26) from the path integral representation of $\mathcal{Z}_{n^q-1, m}$. We consider the $\{q = 3, n = 3, m = 2\}$ case as an example. Replica trick in FIG. 10 is determined by six twist

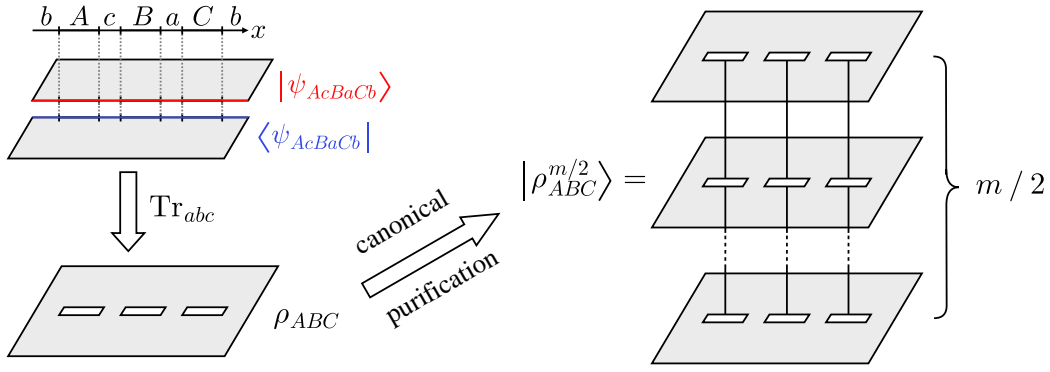


FIG. 9. Left: The path integral representation of the reduced density matrix ρ_{ABC} . Right: The path integral representation of $|\rho_{ABC}^{m/2}\rangle$, which is obtained from the canonical purification of ρ_{ABC} . Here m should be even and it will be analytically continued to 1 in the end.

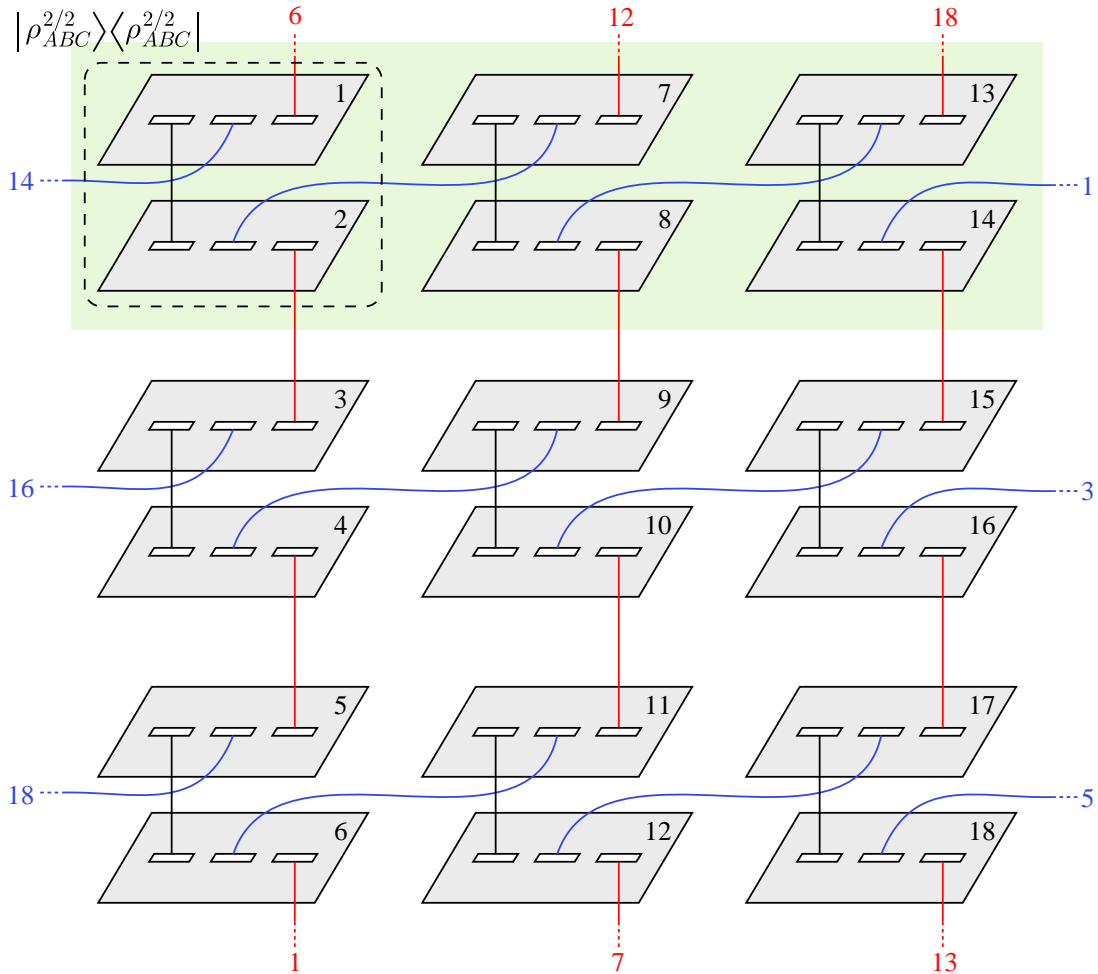


FIG. 10. The path integral representation of $\mathcal{Z}_{nq-1, m}$. Here we take $q = 3$, $n = 3$ and $m = 2$. The part inside the black dashed box is the density matrix $|\rho_{ABC}^{2/2}\rangle\langle\rho_{ABC}^{2/2}|$. In order to make the diagram clear, we omitted some gluing. For example, the black vertical line in the box denotes that the lower edge of subsystem A in the 1st copy is glued to the upper edge of A in the 2nd copy and we omit the line denoting the gluing between the upper edge of A in the 1st copy and the lower edge of A in the 2nd copy. For $m = 2$, if the lower edge of a subsystem in the i -th copy is glued to the upper edge of this subsystem in the j -th copy, the reverse is always true.

operators $\sigma_{i=1,\dots,6}$ located at the endpoints of the subsystems A, B, C as shown in the top left corner of FIG. 9.

These twist operators are made up of three nontrivial operators $\Sigma_{A,B,C}$ associated with the three subsystems A, B, C respectively, which can be described by representation of cyclic groups. For instance, (123) in Σ_A means

$$\begin{aligned}\Sigma_A &= (1, 2)(3, 4)(5, 6)(7, 8)(9, 10)(11, 12)(13, 14)(15, 16)(17, 18) ; \\ \Sigma_B &= (2, 7)(8, 13)(14, 1)(4, 9)(10, 15)(16, 3)(6, 11)(12, 17)(18, 5) ; \\ \Sigma_C &= (2, 3)(4, 5)(6, 1)(8, 9)(10, 11)(12, 7)(14, 15)(16, 17)(18, 13) .\end{aligned}\tag{A1}$$

Then we have

$$\sigma_1 = \Sigma_A , \quad \sigma_2 = \Sigma_A^{-1} , \quad \sigma_3 = \Sigma_B , \quad \sigma_4 = \Sigma_B^{-1} , \quad \sigma_5 = \Sigma_C , \quad \sigma_6 = \Sigma_C^{-1} .\tag{A2}$$

Therefore, the conformal weights of σ_i is⁶ $h_i = (c/24)(2 - 1/2) \times 9$, which is consistent with (25). For general $\{\mathbf{q}, n, m\}$, since there are only m -cycles in $\sigma_{i=1,\dots,6}$, the conformal weight of h_i is thus given by (25).

From (A1) and (A2), we can obtain leading operator $\sigma_{a=16,23,45}$ in the OPE of σ_i and σ_j

$$\begin{aligned}\sigma_{16} &= \sigma_1 \sigma_6 = \Sigma_A \Sigma_C^{-1} = (1, 5, 3)(2, 4, 6)(7, 11, 9)(8, 10, 12)(13, 17, 15)(14, 16, 18) ; \\ \sigma_{23} &= \sigma_2 \sigma_3 = \Sigma_A^{-1} \Sigma_B = (1, 13, 7)(2, 8, 14)(3, 15, 9)(4, 10, 16)(5, 17, 11)(6, 12, 18) ; \\ \sigma_{45} &= \sigma_4 \sigma_5 = \Sigma_B^{-1} \Sigma_C = (1, 11, 15)(2, 16, 12)(3, 7, 17)(4, 18, 8)(5, 9, 13)(6, 14, 10) .\end{aligned}\tag{A3}$$

Therefore, the conformal weights of σ_a are $h_a = (c/24)(3 - 1/3) \times 6$, which is consistent with (26). Now we generalize this result to general $\{\mathbf{q}, n, m\}$ case, where we have mn^{q-1} copies and they form a $\underbrace{n \times n \times \dots \times n}_{q-1}$ lattice with m

copies at each cell point. We focus on the row containing the first cell point⁷ and consider the product of the parts of Σ_A^{-1} and Σ_B restricted to the cell points in this row. We use $\tilde{\Sigma}_A$ and $\tilde{\Sigma}_B$ to denote the parts of Σ_A and Σ_B restricted to this row, and they are given by (since m is even, here we take $m = 2\ell$)

$$\begin{aligned}\tilde{\Sigma}_A &= (1, 2, \dots, \ell, \ell + 1, \ell + 2, \dots, 2\ell)(nm + 1, nm + 2, \dots, nm + \ell, nm + \ell + 1, nm + \ell + 2, \dots, nm + 2\ell) \\ &\quad (2nm + 1, \dots, 2nm + 2\ell) \cdots ((n - 1)nm + 1, \dots, (n - 1)nm + 2\ell) , \\ \tilde{\Sigma}_B &= (\ell + 1, \ell + 2, \dots, 2\ell, nm + 1, nm + 2, \dots, nm + \ell)(nm + \ell + 1, \dots, nm + 2\ell, 2nm + 1, \dots, 2nm + \ell) \cdots \\ &\quad ((n - 2)nm + \ell + 1, \dots, (n - 2)nm + 2\ell, (n - 1)nm + 1, \dots, (n - 1)nm + \ell) \\ &\quad ((n - 1)nm + \ell + 1, \dots, (n - 1)nm + 2\ell, 1, \dots, \ell) .\end{aligned}\tag{A4}$$

The product $\tilde{\Sigma}_A^{-1} \tilde{\Sigma}_B$ is

$$\tilde{\Sigma}_A^{-1} \tilde{\Sigma}_B = (\ell, (n - 1)nm + \ell, (n - 2)nm + \ell, \dots, nm + \ell)(2\ell, nm + 2\ell, 2nm + 2\ell, \dots, (n - 1)nm + 2\ell) ,\tag{A5}$$

which contains two n -cycles. One can check that when $n = 3, m = 2$, (A4) and (A5) reduces to (part of) (A1) and (A3). Note that our analysis here is restricted to a single row. Since there are n^{q-2} rows in total, the

complete $\Sigma_A^{-1} \Sigma_B$ operator consists of $2n^{q-2}$ n -cycles, resulting in the conformal weight (26).

From FIG. 10 we can read

Appendix B: Numerical computation of the six-point function (27)

In this appendix we give a numerical calculation of the six point function (27) with the six points located at x_i (19) and the relevant conformal weights given by (25)

⁶ The conformal weight of twist operator is given by [49]

$$h = \frac{c}{24} \sum_k p_k \left(k - \frac{1}{k} \right) ,$$

with p_k the number of k -cycles.

⁷ This row contains nm replicas in total. For $n = 3$ and $m = 2$ case, this row corresponds to the green shaded part in FIG. 10.

and (26). Utilizing the conformal transformation

$$x_i \rightarrow z_i = \frac{(x_i - x_2)(x_1 - x_6)}{(x_2 - x_6)(x_i - x_1)}, \quad (\text{B1})$$

$\{x_1, x_2, x_6\}$ are mapped to $\{z_1, z_2, z_6\} = \{\infty, 0, 1\}$ while $\{x_3, x_4, x_5\}$ are sent to $\{z_3, z_4, z_5\}$. At the large c limit with $h_{i=1,\dots,6}/c$ and $h_{a=16,23,45}/c$ fixed (here h_i denotes the conformal weight of the external operator $\sigma_i(x_i)$ and h_a the weight of the internal operator), the six point function

$$\langle \sigma_1(z_1) \sigma_2(z_2) \sigma_3(z_3) \sigma_4(z_4) \sigma_5(z_5) \sigma_6(z_6) \rangle \quad (\text{B2})$$

can be approximated by

$$\langle \sigma_1(z_1) \sigma_2(z_2) \sigma_3(z_3) \sigma_4(z_4) \sigma_5(z_5) \sigma_6(z_6) \rangle \approx c_{1,6}^{16} c_{2,3}^{23} c_{4,5}^{45} c_{16,23}^{45} \mathcal{F}(z_i) \mathcal{F}(\bar{z}_i), \quad (\text{B3})$$

where $a = 16, 23, 45$ labels the leading order primary with conformal wight (26), $c_{i,j}^a$ is the OPE coefficient, and \mathcal{F} is the six-point Virasoro block, which exponentiates at large c limit [45]

$$\mathcal{F} \sim \exp \left[-\frac{c}{6} f \left(\frac{h_a}{c}, \frac{h_i}{c}, z_i \right) \right]. \quad (\text{B4})$$

Here f is called the semiclassical block, which can be obtained by solving the following monodromy problem. Consider the second-order differential equation

$$\psi''(z) + T(z)\psi(z) = 0, \quad (\text{B5})$$

where $T(z)$ is given by

$$T(z) = \sum_{i=1}^6 \left(\frac{6h_i/c}{(z-z_i)^2} - \frac{c_i}{z-z_i} \right), \quad (\text{B6})$$

with c_i the accessory parameters satisfying

$$\begin{aligned} \sum_{i=1}^6 c_i &= 0, \\ \sum_{i=1}^6 (c_i z_i - 6h_i/c) &= 0, \\ \sum_{i=1}^6 (c_i z_i^2 - 12z_i h_i/c) &= 0, \end{aligned} \quad (\text{B7})$$

which guarantee that $T(z)$ vanishes as z^{-4} at infinity. As a second-order differential equation, (B5) has two solutions ψ_1 and ψ_2 . Taking these solutions on a closed

contour around some singular point, they will undergo some monodromy

$$\begin{pmatrix} \psi_1 \\ \psi_2 \end{pmatrix} \rightarrow M \begin{pmatrix} \psi_1 \\ \psi_2 \end{pmatrix}. \quad (\text{B8})$$

The accessory parameters c_i can be determined by (B7) and the following three equations

$$\text{Tr} M_a = -2 \cos \left(\pi \sqrt{1 - \frac{24}{c} h_a} \right), \quad a = 16, 23, 45, \quad (\text{B9})$$

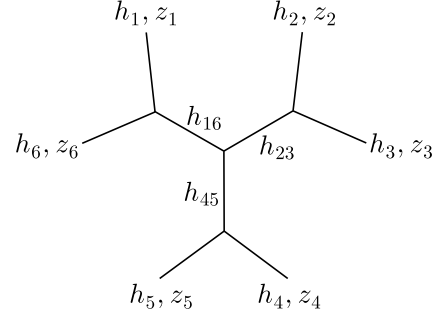


FIG. 11. Dominant fusion channel of the six-point function (B2).

where $M_{a=16}$ denotes the 2×2 monodromy matrix for the cycle γ_{16} enclosing z_1 and z_6 , and similarly for $a = 23, 45$; h_{16} is the conformal weight of the leading operator in the OPE contraction of $\sigma_1(z_1)$ and $\sigma_6(z_6)$ as shown in FIG. 11, similarly for $a = 23, 45$. From (25) we know that $h_{16} = h_{23} = h_{45} = \frac{c}{12} (n^2 - 1)$.

The relation between the semi-classical block f and the accessory parameters c_i are

$$\partial f / \partial z_i = c_i. \quad (\text{B10})$$

Therefore, we can calculate the partial derivative of $S_R^{(q)}$ with respect to the coordinate parameters $\xi = a, b, r$ in (19). From (24), (27) and (B3) we obtain

$$\begin{aligned} \frac{\partial S_R^{(q)}}{\partial \xi} &= \lim_{n \rightarrow 1} \frac{1}{n-1} \frac{c}{3} \sum_{i=1}^6 \frac{\partial f}{\partial z_i} \frac{\partial z_i}{\partial \xi} \\ &= \lim_{n \rightarrow 1} \frac{1}{n-1} \frac{c}{3} \sum_{i=1}^6 c_i \frac{\partial z_i}{\partial \xi}. \end{aligned} \quad (\text{B11})$$

- [1] R. Horodecki, P. Horodecki, M. Horodecki, and K. Horodecki, Quantum entanglement, *Rev. Mod. Phys.* **81**, 865 (2009), [arXiv:quant-ph/0702225](#).
- [2] L. Amico, R. Fazio, A. Osterloh, and V. Vedral, Entanglement in many-body systems, *Rev. Mod. Phys.* **80**, 517 (2008), [arXiv:quant-ph/0703044](#).
- [3] J. M. Maldacena, The Large N limit of superconformal

field theories and supergravity, *Adv. Theor. Math. Phys.* **2**, 231 (1998), [arXiv:hep-th/9711200](#).

- [4] S. S. Gubser, I. R. Klebanov, and A. M. Polyakov, Gauge theory correlators from noncritical string theory, *Phys. Lett. B* **428**, 105 (1998), [arXiv:hep-th/9802109](#).
- [5] E. Witten, Anti-de Sitter space and holography, *Adv. Theor. Math. Phys.* **2**, 253 (1998), [arXiv:hep-th/9802150](#).

- [6] S. Ryu and T. Takayanagi, Holographic derivation of entanglement entropy from AdS/CFT, *Phys. Rev. Lett.* **96**, 181602 (2006), [arXiv:hep-th/0603001](#).
- [7] S. Ryu and T. Takayanagi, Aspects of Holographic Entanglement Entropy, *JHEP* **08**, 045, [arXiv:hep-th/0605073](#).
- [8] V. E. Hubeny, M. Rangamani, and T. Takayanagi, A Covariant holographic entanglement entropy proposal, *JHEP* **07**, 062, [arXiv:0705.0016 \[hep-th\]](#).
- [9] A. C. Wall, Maximin Surfaces, and the Strong Subadditivity of the Covariant Holographic Entanglement Entropy, *Class. Quant. Grav.* **31**, 225007 (2014), [arXiv:1211.3494 \[hep-th\]](#).
- [10] T. Takayanagi and K. Umemoto, Entanglement of purification through holographic duality, *Nature Phys.* **14**, 573 (2018), [arXiv:1708.09393 \[hep-th\]](#).
- [11] P. Nguyen, T. Devakul, M. G. Halbasch, M. P. Zaletel, and B. Swingle, Entanglement of purification: from spin chains to holography, *JHEP* **01**, 098, [arXiv:1709.07424 \[hep-th\]](#).
- [12] P. Caputa, M. Miyaji, T. Takayanagi, and K. Umemoto, Holographic Entanglement of Purification from Conformal Field Theories, *Phys. Rev. Lett.* **122**, 111601 (2019), [arXiv:1812.05268 \[hep-th\]](#).
- [13] S. Dutta and T. Faulkner, A canonical purification for the entanglement wedge cross-section, *JHEP* **03**, 178, [arXiv:1905.00577 \[hep-th\]](#).
- [14] H.-S. Jeong, K.-Y. Kim, and M. Nishida, Reflected Entropy and Entanglement Wedge Cross Section with the First Order Correction, *JHEP* **12**, 170, [arXiv:1909.02806 \[hep-th\]](#).
- [15] P. Hayden, O. Parrikar, and J. Sorce, The Markov gap for geometric reflected entropy, *JHEP* **10**, 047, [arXiv:2107.00009 \[hep-th\]](#).
- [16] J. Kudler-Flam and S. Ryu, Entanglement negativity and minimal entanglement wedge cross sections in holographic theories, *Phys. Rev. D* **99**, 106014 (2019), [arXiv:1808.00446 \[hep-th\]](#).
- [17] Y. Kusuki, J. Kudler-Flam, and S. Ryu, Derivation of holographic negativity in AdS₃/CFT₂, *Phys. Rev. Lett.* **123**, 131603 (2019), [arXiv:1907.07824 \[hep-th\]](#).
- [18] X. Dong, X.-L. Qi, and M. Walter, Holographic entanglement negativity and replica symmetry breaking, *JHEP* **06**, 024, [arXiv:2101.11029 \[hep-th\]](#).
- [19] X. Dong, S. McBride, and W. W. Weng, Replica wormholes and holographic entanglement negativity, *JHEP* **06**, 094, [arXiv:2110.11947 \[hep-th\]](#).
- [20] X. Dong, J. Kudler-Flam, and P. Rath, Entanglement Negativity and Replica Symmetry Breaking in General Holographic States, (2024), [arXiv:2409.13009 \[hep-th\]](#).
- [21] K. Tamaoka, Entanglement Wedge Cross Section from the Dual Density Matrix, *Phys. Rev. Lett.* **122**, 141601 (2019), [arXiv:1809.09109 \[hep-th\]](#).
- [22] A. Mollabashi and K. Tamaoka, A Field Theory Study of Entanglement Wedge Cross Section: Odd Entropy, *JHEP* **08**, 078, [arXiv:2004.04163 \[hep-th\]](#).
- [23] M. Walter, D. Gross, and J. Eisert, Multi-partite entanglement, (2016), [arXiv:1612.02437 \[quant-ph\]](#).
- [24] S. Nezami and M. Walter, Multipartite Entanglement in Stabilizer Tensor Networks, *Phys. Rev. Lett.* **125**, 241602 (2020), [arXiv:1608.02595 \[quant-ph\]](#).
- [25] Y. Zou, K. Siva, T. Soejima, R. S. K. Mong, and M. P. Zaletel, Universal tripartite entanglement in one-dimensional many-body systems, *Phys. Rev. Lett.* **126**, 120501 (2021), [arXiv:2011.11864 \[quant-ph\]](#).
- [26] C. A. Agón, P. Bueno, O. Lasso Andino, and A. Villar López, Aspects of N-partite information in conformal field theories, *JHEP* **03**, 246, [arXiv:2209.14311 \[hep-th\]](#).
- [27] G. Penington, M. Walter, and F. Witteveen, Fun with replicas: tripartitions in tensor networks and gravity, *JHEP* **05**, 008, [arXiv:2211.16045 \[hep-th\]](#).
- [28] V. E. Hubeny, M. Rangamani, and M. Rota, The holographic entropy arrangement, *Fortsch. Phys.* **67**, 1900011 (2019), [arXiv:1812.08133 \[hep-th\]](#).
- [29] T. He, M. Headrick, and V. E. Hubeny, Holographic Entropy Relations Repackaged, *JHEP* **10**, 118, [arXiv:1905.06985 \[hep-th\]](#).
- [30] S. Hernández-Cuenca, V. E. Hubeny, and H. F. Jia, Holographic entropy inequalities and multipartite entanglement, *JHEP* **08**, 238, [arXiv:2309.06296 \[hep-th\]](#).
- [31] K. Umemoto and Y. Zhou, Entanglement of Purification for Multipartite States and its Holographic Dual, *JHEP* **10**, 152, [arXiv:1805.02625 \[hep-th\]](#).
- [32] N. Bao and I. F. Halpern, Conditional and Multipartite Entanglements of Purification and Holography, *Phys. Rev. D* **99**, 046010 (2019), [arXiv:1805.00476 \[hep-th\]](#).
- [33] N. Bao and N. Cheng, Multipartite Reflected Entropy, *JHEP* **10**, 102, [arXiv:1909.03154 \[hep-th\]](#).
- [34] J. Chu, R. Qi, and Y. Zhou, Generalizations of Reflected Entropy and the Holographic Dual, *JHEP* **03**, 151, [arXiv:1909.10456 \[hep-th\]](#).
- [35] A. Gadde, V. Krishna, and T. Sharma, New multipartite entanglement measure and its holographic dual, *Phys. Rev. D* **106**, 126001 (2022), [arXiv:2206.09723 \[hep-th\]](#).
- [36] A. Gadde, V. Krishna, and T. Sharma, Towards a classification of holographic multi-partite entanglement measures, *JHEP* **08**, 202, [arXiv:2304.06082 \[hep-th\]](#).
- [37] A. Gadde, S. Jain, V. Krishna, H. Kulkarni, and T. Sharma, Monotonicity conjecture for multi-party entanglement. Part I, *JHEP* **02**, 025, [arXiv:2308.16247 \[hep-th\]](#).
- [38] J. Harper, T. Takayanagi, and T. Tsuda, Multi-entropy at low Renyi index in 2d CFTs, *SciPost Phys.* **16**, 125 (2024), [arXiv:2401.04236 \[hep-th\]](#).
- [39] A. Gadde, S. Jain, and H. Kulkarni, Multi-partite entanglement monotones, (2024), [arXiv:2406.17447 \[quant-ph\]](#).
- [40] C. Holzhey, F. Larsen, and F. Wilczek, Geometric and renormalized entropy in conformal field theory, *Nucl. Phys. B* **424**, 443 (1994), [arXiv:hep-th/9403108](#).
- [41] P. Calabrese and J. L. Cardy, Entanglement entropy and quantum field theory, *J. Stat. Mech.* **0406**, P06002 (2004), [arXiv:hep-th/0405152](#).
- [42] P. Calabrese and J. Cardy, Entanglement entropy and conformal field theory, *J. Phys. A* **42**, 504005 (2009), [arXiv:0905.4013 \[cond-mat.stat-mech\]](#).
- [43] A. A. Belavin, A. M. Polyakov, and A. B. Zamolodchikov, Infinite Conformal Symmetry in Two-Dimensional Quantum Field Theory, *Nucl. Phys. B* **241**, 333 (1984).
- [44] A. B. Zamolodchikov, Conformal symmetry in two-dimensional space: Recursion representation of conformal block, *Theor. Math. Phys.* **73**, 1088 (1987).
- [45] T. Hartman, Entanglement Entropy at Large Central Charge, (2013), [arXiv:1303.6955 \[hep-th\]](#).
- [46] M. Banados, C. Teitelboim, and J. Zanelli, The Black hole in three-dimensional space-time, *Phys. Rev. Lett.* **69**, 1849 (1992), [arXiv:hep-th/9204099](#).
- [47] T. Barrella, X. Dong, S. A. Hartnoll, and V. L. Mar-

- tin, Holographic entanglement beyond classical gravity, *JHEP* **09**, 109, [arXiv:1306.4682 \[hep-th\]](#).
- [48] T. Faulkner, A. Lewkowycz, and J. Maldacena, Quantum corrections to holographic entanglement entropy, *JHEP* **11**, 074, [arXiv:1307.2892 \[hep-th\]](#).
- [49] O. Lunin and S. D. Mathur, Correlation functions for $M^2 \times N / S(N)$ orbifolds, *Commun. Math. Phys.* **219**, 399 (2001), [arXiv:hep-th/0006196](#).